

MOL2774

## Mapping of maurotoxin binding sites on hKv1.2, hKv1.3 and hIKCa1 channels

Violeta Visan, Ziad Fajloun, Jean-Marc Sabatier, Stephan Grissmer<sup>✉</sup>

University of Ulm, Dept. of Applied Physiology, Albert-Einstein-Allee 11, Germany  
(VV, SG)

Laboratoire International Associé d'Ingénierie Biomoléculaire, CNRS UMR 6560, Bd  
Pierre Dramard, 13916 Marseille Cedex 20, France (ZF, JMS)

MOL2774

**Running title:** Mapping of maurotoxin binding sites on potassium channels

Number of text pages: 33

Number of tables: 0

Number of figures: 9

Number of references: 40

Number of words in: Abstract: 222

Introduction: 622

Discussion: 1381

**List of non-standard abbreviation:**

hKv1.2 and hKv1.3: human voltage-activated potassium channels

hKCa1: human intermediate-conductance calcium-activated potassium channels

MTX: maurotoxin

CTX: charybdotoxin

AgTx2: agitoxin 2

KTX: kaliotoxin

✉ Correspondence should be addressed to

Professor Dr. Stephan Grissmer

Department of Applied Physiology

University of Ulm

Albert-Einstein-Allee 11

D-89081 Ulm, Germany

Tel.: (0049) 731 502 32 53

Fax.: (0049) 731 502 32 37

e-mail: [stephan.grissmer@medizin.uni-ulm.de](mailto:stephan.grissmer@medizin.uni-ulm.de)

MOL2774

## Abstract

Maurotoxin (MTX) is a potent blocker of human voltage-activated Kv1.2 and intermediate-conductance calcium-activated potassium channels, hKCa1. Since its blocking affinity on both channels is similar, although the pore region of these channels show only few conserved amino acids, we aimed to characterize the binding sites of MTX in these channels. Investigating the  $\text{pH}_o$  dependency of MTX block on current through hKv1.2 channels, we concluded that the block is less  $\text{pH}_o$  sensitive than for hKCa1 channels. Using mutant cycle analysis and computer docking we tried to identify the amino acids through which MTX binds to hKv1.2 and hKCa1 channels. We report that MTX interacts with hKv1.2 mainly through six strong interactions. Lys<sup>23</sup> from MTX protrudes into the channel pore interacting with the GYGD motif, while Tyr<sup>32</sup> and Lys<sup>7</sup> interact with Val<sup>381</sup>, Asp<sup>363</sup>, and Glu<sup>355</sup>, stabilising the toxin onto the channel pore. Since only Val<sup>381</sup>, Asp<sup>363</sup>, and the GYGD motif are conserved in hKCa1 channels, and the replacement of His<sup>399</sup> from hKv1.3 channels with a threonine makes this channel MTX sensitive, we concluded that MTX binds to all three channels through the same amino acids, Glu<sup>355</sup>, although important, being not essential in MTX recognition. A negatively charged amino acid in this position could better stabilize the toxin-channel interaction, and could explain the  $\text{pH}_o$  sensitivity of MTX block on current through hKCa1 versus hKv1.2 channels.

## INTRODUCTION

It is well recognized that scorpion venoms represent important sources of potassium channels peptide blockers. Interactions between scorpion toxins and potassium channels were investigated in numerous studies and provided insights into the structure and topology of the external pore vestibule of the channels (Hidalgo and Mac Kinnon, 1995; Aiyar et al., 1996; Rauer et al., 2000, Wrisch and Grissmer, 2000).

Maurotoxin (MTX) is a scorpion toxin isolated recently from the venom of the Tunisian chactoid scorpion *Scorpio maurus palmatus* (Kharrat et al., 1996, 1997; Castle et al., 2003). It belongs to the  $\alpha$ -KTX toxins family (Tytgat et al., 1999) (Fig. 1B). It is composed by 34 amino acids peptide and has four disulfide bridges with an atypical pattern organisation (C1-C5, C2-C6, C3-C4, and C7-C8) compared with other toxins belonging to the same family (C1-C4, C2-C5, C3-C6 for three-disulfide bridged toxins and C1-C5, C2-C6, C3-C7, and C4-C8 for four-disulfide bridged toxins) (Kharrat et al., 1996). Despite its different disulfide bridges organisation, MTX has the same three dimensional structure of potassium channels toxin blockers formed by one  $\alpha$ -helix and two  $\beta$ -sheets. Moreover, MTX was described to block, in *Xenopus laevis* oocytes, IKCa1, Kv1.2, and ShakerB channels with an affinity lower than 10 nM, whereas its affinity for other potassium channels as Kv1.1 and Kv1.3 was higher than 50 nM (Kharrat et al., 1996; Lecomte et al., 2000; Avdonin et al., 2000; Castle et al., 2003).

hKv1.2 and hIKCa1 channels are differently distributed in a variety of tissues. hKv1.2 channels are found predominantly in the brain where they are most likely associated with Kv1.1 and Kv1.6 channel subunits accomplishing crucial roles in neuronal signal transmission (Coleman et al., 1999; Monaghan et al., 2001; Dodson et

MOL2774

al., 2003). In contrast, hIKCa1 channels are not expressed in brain, however, they play important functions in many peripheral tissues and cells like erythrocytes, human T-lymphocytes, and colon (Grissmer et al., 1993; Ishii et al., 1997; Logsdon et al., 1997; Vandorpe et al., 1998; Ghanshani et al., 2000; Chandy et al., 2001). Since their up-regulation was associated with cell proliferation, hIKCa1 channels were designated as therapeutic targets and, possibly, markers of physiological and pathological cell proliferation (Vandorpe et al., 1998; Khanna et al., 1999; Pena and Rane, 1999; Wulff et al., 2000; Rane, 2000; Kohler et al., 2000; Elliot and Higgins, 2003; Jäger et al., 2004). In our study we aimed to find all the interactions of MTX with hKv1.2 and hIKCa1 channels, and to investigate the possibility of designing future MTX derivatives that would discriminate these two channels.

To identify the molecular determinants that are responsible for the binding specificity of MTX to hIKCa1 and hKv1.2 channels, we used as approach the thermodynamic mutant cycle analysis as described by Schreiber and Fersht (1995), and Hidalgo and Mac Kinnon (1995). Thermodynamic mutant cycles assist in studying of coupling energies between pairs of amino acids in a protein-protein complex. The dimensionless  $\Omega$  value indicates the interaction strength of a given channel-toxin pair and can be calculated using toxin half-blocking doses. The change in coupling energy  $\Delta\Delta G$  can then be calculated ( $\Delta\Delta G = kT \ln \Omega$ ). The distances between this pair of residues can then be estimated based on the studies of Schreiber and Fersht (1995) and Hidalgo and MacKinnon (1995) assuming that  $\Delta\Delta G$  values  $\geq 0.5$  kcal/mol correspond to an inter-residue distance of  $< 5$  Å. Since hKv1.2 and hIKCa1 channels show many structural similarities in the pore region with hKv1.3 channels (Fig. 1A), although these channels are not MTX sensitive, we compared the binding sites of MTX in all three channels. Thus, this study helped us to better understand the mechanism of MTX

MOL2774

block on potassium channels, and to propose a docking model of MTX into the pore of hKv1.2 channel.

## MATERIALS AND METHODS

**Cells.** The COS-7 cell line was maintained in DMEM with Earle's salts (Gibco, UK), and 10% heat-inactivated FCS. Cells were kept in an humidified, 10% CO<sub>2</sub> incubator at 37 °C.

**Solutions.** All experiments were carried out at room temperature (21-25 °C). Cells were measured in normal mammalian Ringer's solution containing (in mM): 160 NaCl, 4.5 KCl, 2 CaCl<sub>2</sub>, 1 MgCl<sub>2</sub>, and 10 HEPES, with an osmolarity of 290-320 mOsm. The pH<sub>o</sub> was adjusted to 7.4 with NaOH. A simple syringe-driven perfusion system was used to exchange the bath solution in the recording chamber. The internal pipette solution used for measuring hKv1.2 and hKv1.3 currents contained (in mM): 155 KF, 2 MgCl<sub>2</sub>, 10 EGTA, 10 HEPES and for measuring Ca<sup>2+</sup>-activated potassium currents: 135 K-aspartate, 8.7 CaCl<sub>2</sub>, 2 MgCl<sub>2</sub>, 10 EGTA, 10 HEPES (free [Ca<sup>2+</sup>]<sub>i</sub> = 10<sup>-6</sup> M), in both solutions the pH was adjusted to 7.2 with KOH, and had osmolarities between 290 and 320 mOsm.

**Toxins.** MTX and related analogs were chemically produced by the solid-phase technique (Merrifield, 1986) using a peptide synthesizer (Model 433A, Applied Biosystems Inc.). Peptide chains were assembled stepwise on 0.3 mequiv. of Fmoc-amide resin (0.68 mequiv. of amino group/g) using 1 mmol of N-a-fluorenylmethyloxycarbonyl (Fmoc) amino acid derivatives. The side chain-protecting groups used for trifunctional residues were: trityl for Cys, Asn, and Gln; tert-butyl for Ser, Thr, Tyr, and Asp; pentamethylchroman for Arg, and tert-butyloxycarbonyl for Lys. The Fmoc-amino acid derivatives were coupled for 20 min as their hydroxybenzotriazole active esters in N-methylpyrrolidinone (3.3-fold excess). The peptide resins (ca. 2.5g) were treated for 2.5 h at 25°C with a mixture of trifluoroacetic

MOL2774

acid/H<sub>2</sub>O/thioanisole/ethanedithiol (88:5:5:2, v/v) in the presence of phenol (2.5 g). The reduced peptides were oxidized/folded at approx. 2 mM peptide concentration in 200 mM Tris/HCl buffer, pH 8.3 (72 h, 25°C), and purified by reversed-phase high-pressure liquid chromatography (HPLC) (Perkin-Elmer, C18 Aquapore ODS 20 mm, 250 x 10 mm) by means of a 60-min linear gradient of 0.08% (v/v) trifluoroacetic acid (TFA)/ 0% to 35% acetonitrile in 0.1% (v/v) TFA/H<sub>2</sub>O at a flow rate of 6 ml/min ( $\lambda$  = 230 nm). The peptides were finally characterized for homogeneity (> 99%) and identity by analytical C18 reversed-phase HPLC, amino acid analysis, Edman sequencing, and mass spectrometry.

Charybdotoxin (CTX) was obtained from Bachem Biochemica GmbH (Heidelberg, Germany). All lyophilized peptides were kept at –20 °C, and the final dilutions were prepared before the measurements in normal Ringer's solution containing 0.1 % bovine serum albumin.

**Electrophysiology.** All the experiments were carried out using the whole-cell recording mode of the patch-clamp technique (Hamill et al., 1981; Rauer and Grissmer, 1996). Electrodes were pulled from glass capillaries (Science Products, Germany) in three stages, and fire-polished to resistances measured in the bath of 2.5–5 M $\Omega$ . Membrane currents were measured with an EPC-9 patch-clamp amplifier (HEKA Elektronik, Lambrecht, Germany) interfaced to a Macintosh computer running the acquisition and analysis software Pulse and PulseFit (HEKA Elektronik, Lambrecht, Germany). The holding potential in all experiments was –80 mV. Series resistance compensation (80%) was used when currents were bigger than 2 nA. When current exceeded 15 nA membrane patches were pulled, and measurements were performed in the outside-out configuration. Data analysis was performed in IgorPro 3.1 (WaveMetrics, Oregon, USA), and  $K_d$  values were deduced by fitting a modified



MOL2774

Hill equation ( $X_{\text{toxin}}/X_{\text{control}} = 1/[1 + ([\text{toxin}]/K_d)]$ , where X is the peak current (for hKv1.2 and hKv1.3 channels), or the slope of the ramp current, i. e. the conductance, measured between -100 and -60 mV (for hIKCa1 channels)) to the normalized data points obtained at more than four different toxin concentrations. This fit indicates that one toxin molecule is sufficient to block the current through the channel. The standard deviations obtained by this fitting routine reflect the uncertainty of the fit. When  $K_d$  was deduced from one single concentration the following calculation was used:  $K_d = [\text{toxin}]/((1/y)-1)$ , where y is the fraction of unblocked peak current or conductance. The value of each toxin concentration was the mean of at least three measurements  $\pm$  SD (where SD represent the standard deviations of the calculated  $K_d$  values).

**Transfection.** pcDNA3/Hygro vectors containing the entire coding sequence of hKv1.2, or hIKCa1, or pRCMV vector containing the coding sequence of hKv1.3 (a kind gift from Dr. O. Pongs, University of Hamburg, Germany) were co-transfected together with a GFP expressing construct into COS-7 cells using FuGene6 Transfection Reagent (Roche, Germany), and currents were measured 2-3 days after transfection.

**Mutagenesis.** All the hKv1.2 (R354A, E355A, D363A, V381A, V381H, and T383A), and hIKCa1 (D239N) channel mutants were generated with the QuickChange<sup>TM</sup> site-directed mutagenesis kit (Stratagene, Germany), and the mutations were confirmed by sequencing (GATC, Germany). The hKv1.3 (H399T) channel mutant was generated by T. Dreker (University of Ulm, Germany).

**Double mutant cycle analysis.** This method was extensively used to assess the distances that lie between two interacting amino acids by estimating their strength of interaction. The change in the coupling energy of interaction is given by  $\Delta\Delta G = kT \ln(\Omega)$ , where k is the Boltzmann constant, T is the temperature, and  $\Omega$  is calculated

MOL2774

from the  $K_d$  values of the wild type and mutant channels and toxins,  $\Omega = (K_d \text{ (wt channel-wt toxin)} * (K_d \text{ (mutant channel-mutant toxin)}) / (K_d \text{ (wt channel-mut toxin)} * (K_d \text{ (mut channel-wt toxin)}))$ . According to Schreiber and Fersht (1995), and Hidalgo and MacKinnon (1995) if  $\Delta\Delta G$  is  $\geq 0.5$  kcal/mol, the distance between the two investigated amino acids is smaller than 5 Å.

**Docking.** For the docking of MTX into the hKv1.2 channel vestibule we used the crystal structure of the KcsA channel (Doyle et al., 1998) and the KvAP channel (Jiang et al., 2003). The homology model of the hKv1.2 channel was made by replacing the KcsA amino acids with the equivalent amino acids from the hKv1.2 channel sequence. The docking was performed manually by fitting the MTX into the channel pore similar to the docking of KTX into the mKv1.1 channel vestibule described by Wrisch and Grissmer (2000). The program used for docking was RasMol v2. The orientation of the toxin into the channel was deduced from the changes in affinity of MTX mutants for the wild type and mutant hKv1.2 channel and mutant cycle analysis.

## RESULTS

Our work attempted to characterize the interaction of a pore blocking toxin, MTX, with hKv1.2 and hIKCa1 channels. Since the block of MTX on current through hIKCa1 channels was reported to be  $\text{pH}_o$  dependent, we investigated the  $\text{pH}_o$  dependence of MTX block on current through hKv1.2 channels. Using mutant cycle analysis we identified several MTX binding sites for hKv1.2 channels, and we proposed a docking model. Additionally, a comparison of the binding sites of MTX for hKv1.2, hIKCa1, and hKv1.3 channels was made.

*MTX blocks both current through hKv1.2, and hIKCa1, but not through Kv1.3 channels.* hKv1.2, hKv1.3, and hIKCa1 channels were expressed in transiently transfected COS-7 cells. The currents through hKv1.2, and hKv1.3 channels were elicited by depolarizing voltage steps of 200 ms from the holding potential  $-80$  mV to  $+40$  mV, whereas hIKCa1 currents were elicited by  $1$   $\mu\text{M}$  internal calcium and 400 ms voltage ramps from  $-120$  mV to  $0$  mV (Fig. 2). To assess the blocking activity of MTX on hKv1.2 and hIKCa1 channels, we applied to the external Ringer solution  $1$  nM MTX for hKv1.2 channels, and  $5$  nM MTX for hIKCa1 channels. These concentrations led to a reduction of almost 50% of both the peak current of hKv1.2 channels (Fig. 2A), and the current conductance of hIKCa1 channels (Fig. 2B). The  $K_d$  values calculated from concentration dose-responses, revealed a half-blocking concentration of  $0.7 \pm 0.1$  nM ( $n = 5$ ) for hKv1.2, and  $4.3 \pm 0.3$  nM ( $n = 6$ ) for hIKCa1, respectively (Fig. 2A, B, bottom). To block current through hKv1.3 channels,  $1$   $\mu\text{M}$  MTX was applied to the external Ringer solution (Fig. 2C). This concentration blocked about 20% of the peak current. Concentration dose-responses allowed us to calculate a  $K_d$  of  $3.3 \pm 0.2$   $\mu\text{M}$  ( $n = 9$ ) (Fig. 2C, bottom).

*The  $pH_o$  dependence of MTX block on current through hKv1.2 channels.* Since MTX block on current through hIKCa1 is  $pH_o$  dependent (Visan et al., 2004), and several reports made by now indicate an increase (Deutsch et al., 1991; Perez-Cornejo et al., 1998) or a decrease (Wrisch and Grissmer, 2000) of peptide binding affinities by an increase in  $pH_o$  values, we investigated the  $pH_o$  dependence of MTX block on current through hKv1.2 channels. We applied 1 nM of MTX to the extracellular Ringer solution, and we deduced the  $K_d$  values of MTX block from single concentration calculations as described in the Methods. At  $pH_o$  7.4 the  $K_d$  value of the MTX block is  $0.4 \pm 0.2$  nM ( $n = 5$ ). Fig. 3 shows that the MTX block on current through hKv1.2 channels is not significantly  $pH_o$  dependent at  $pH_o$  values of 6.2 (Fig. 3A), and 8.3 (Fig. 3C), where the  $K_d$  values are  $0.6 \pm 0.3$  nM ( $n = 7$ ), and  $0.6 \pm 0.3$  nM ( $n = 4$ ), respectively. However, for  $pH_o$  values of 9.1 the block of MTX on current through hKv1.2 channels is about two-three fold weaker ( $K_d = 1.2 \pm 0.5$  nM ( $n = 4$ )) (Fig. 3D).

To test if the  $pH_o$  affects the binding affinities of other pore blocking peptides we investigated the  $pH_o$  dependency of charybdotoxin (CTX) (Lambert et al., 1990) block on current through hKv1.2 channels. A concentration of 20 nM CTX blocked around 50 % of the peak current at  $pH_o$  7.4 (Fig. 4B). This concentration was further used to calculate the  $K_d$  according to the equation described in the Methods. As Fig. 4 shows, CTX blocked the current through hKv1.2 channels with similar potency in  $pH_o$  6.2, 7.4, 8.3, and 9.1 ( $K_d$  values being  $23 \pm 2$  nM ( $n = 6$ ),  $19 \pm 2$  nM ( $n = 4$ ),  $24 \pm 6$  nM ( $n = 6$ ), and  $25 \pm 4$  nM ( $n = 6$ ), respectively). These results would confirm the theory that higher  $pH_o$  values might slightly change the three dimensional structure of MTX, and thus decrease its blocking affinity for hIKCa1 and hKv1.2 channels (see Discussions).

MOL2774

*Important amino acids for MTX-hKv1.2 channel interaction.* To identify the important amino acids in MTX-hKv1.2 interaction, five candidate amino acids from hKv1.2 channel were selected (Fig. 1A, highlighted amino acids), and mutated to alanine or histidine R354A, E355A, D363A, V381A, V381H, and T383A. The selection of these amino acids was made based on computer simulations (Fu et al, 2002), or previous reports of the importance in MTX or other peptide toxins binding of the amino acids situated in equivalent positions in other potassium channels. Thus, it have been reported that the position 381 from hKv1.2 channels is important in ShakerB channels for MTX binding (Thr<sup>499</sup>) (Avdonin et al, 2000), whereas in Kv1.3 channels the correspondent amino acid (His<sup>404</sup>) is important in the binding of TEA (Bretschneider et al, 1999), CTX (Rauer et al, 2000), or KTX (Aiyar et al, 1996). Similarly, position 363 from hKv1.2 channels have been reported as an important position in hKCa1 channels (Asp<sup>239</sup>) for CTX binding (Rauer et al, 2000), while the correspondent amino acid of position 355 from hKv1.2 channels have been shown to have a small influence in KTX binding to Kv1.1 channels (Glu<sup>355</sup>) (Wrisch and Grissmer, 2000). For MTX were selected six of the peripheral amino acids: S6A, K7A, Y10A, R14Q, K23A, and Y32A that have been shown to have influence in MTX binding (Castle et al, 2003). The blocking affinities of MTX or mutant MTX for wild type or modified hKv1.2 channels is represented in Fig. 5A. The only mutation in the channel that drastically modified MTX binding affinity is hKv1.2\_V381H. The replacement of Val<sup>381</sup> with a histidine (the amino acid that corresponds to His<sup>399</sup> from hKv1.3 channel or Tyr<sup>82</sup> from KcsA channel (Fig. 1A)), change MTX blocking affinity more than 350 fold, from  $0.7 \pm 0.1$  nM (n = 5) to  $255 \pm 55$  nM (n = 4). For the other channel mutations MTX blocking affinity was not affected (hKv1.2\_R354A, hKv1.2\_D363A, and hKv1.2\_T383A), or was affected with a less than 10 fold

MOL2774

difference (hKv1.2\_E355A, and hKv1.2\_V381A). MTX mutations affected more the binding affinities of the peptides, with a decrease of more than 1000 fold for MTX\_K23A, and MTX\_Y32A, and around 100 fold for MTX\_R14Q and MTX\_K7A, results that are in agreement with previous studies (Castle et al., 2003). The inferred  $K_d$  values (Fig. 5A) were further used to perform mutant cycle analysis and to calculated the change in coupling energy ( $\Delta\Delta G$ ) between different amino acid pairs (Fig. 5B). The change in coupling energy allowed us to estimate the distance that lie between certain toxin-channel amino acids. If  $\Delta\Delta G$  is  $\geq 0.5$  kcal/mol, the distance between two amino acids is less than 5 Å (Schreiber and Fersht, 1995). The mutation to alanine of the amino acids Ser<sup>6</sup> and Tyr<sup>10</sup> from MTX, and Arg<sup>345</sup> and Thr<sup>383</sup> from hKv1.2 channels apparently did not make a difference in MTX-hKv1.2 interaction since the calculated change in coupling energies between them and different amino acids from the channel/toxin were smaller than 0.5 kcal/mol (Fig. 5B). Two possibilities could account for this. Either the substitution to alanine of these amino acids does not bring a drastic change in coupling energy because alanine has been replaced by amino acids with equally favorable interactions as they occur in the case of the wild type channels/ wild type toxin, or these amino acids do not participate in the interaction. In the following, we focused on the other amino acid residues of which changes in coupling energies were more than 0.49 kcal/mol.

In Fig. 6A, and 6B is represented an example of a significant change in the binding affinity of a mutant toxin, for the hKv1.2 channel. The substitution of K7A makes the toxin almost 100 times less potent for hKv1.2 channels, the  $K_d$  value decreasing from  $0.7 \pm 0.1$  nM ( $n = 5$ ) (for the wild type MTX) to  $59 \pm 4$  nM ( $n = 4$ ) (for MTX\_K7A mutant). Mutant cycle analysis show a change in coupling energy of 0.52 kcal/mol between Lys<sup>7</sup> and Asp<sup>363</sup>, and 0.9 kcal/mol between Lys<sup>7</sup> and Glu<sup>355</sup>

MOL2774

(Fig. 6C) suggesting that Lys<sup>7</sup> is situated in close proximity with these two amino acids, the distance that separate them being less than 5 Å.

A key role in MTX binding seems to have Val<sup>381</sup> from hKv1.2 channel. The calculated  $\Delta\Delta G$  values indicate that Val<sup>381</sup> is in the very close proximity (less than 5 Å) of Lys<sup>7</sup>, Lys<sup>23</sup>, and Tyr<sup>32</sup> from MTX since their changes in coupling energies are bigger than 0.5 kcal/mol (Fig. 6C).

*MTX binding sites for hKCa1 channels.* To test if MTX has the same binding sites for hKCa1 as for hKv1.2 channels, we mutated the Asp<sup>239</sup> to Asn. This amino acid is highly conserved among the Kv1 potassium channel family and corresponds to Asp<sup>363</sup> from hKv1.2 channels and His<sup>399</sup> from hKv1.3 channels (Fig. 1A). Fig. 7A and B show the loss in blocking affinity of MTX\_K7A mutant for hKCa1 channel ( $32 \pm 3$  nM (n = 4) versus  $4.3 \pm 0.3$  nM (n = 6) for the wild type toxin). Mutant cycle analysis reveals a change in coupling energy between Asp<sup>239</sup> and Lys<sup>7</sup> of 0.49 kcal/mol (Fig. 7C), which would indicate a distance between these two amino acids close to 5 Å. These results, together with the drastically loss in affinity of two of the MTX mutants (MTX\_K23A, and MTX\_Y32A) for hKCa1 channels (Castle et al., 2003), and the computer simulations made by Fu et al. (2002) indicate at least three common binding sites of MTX for both hKv1.2 and hKCa1 channels.

*MTX binding sites for hKv1.3 channels.* Since MTX blocks hKv1.3 with very low affinity ( $K_d = 3.3 \pm 0.2$   $\mu$ M (n = 9)) (Fig. 8A), we mutated one amino acid that corresponds to a key binding amino acids in hKv1.2, and we investigated the MTX blocking activity of this mutant channel. His<sup>399</sup> from hKv1.3 corresponds to Val<sup>381</sup> from hKv1.2, Thr<sup>451</sup> from ShakerB channels, and Tyr<sup>82</sup> from KcsA channels (Fig. 1A). Since ShakerB channels are also sensitive to MTX, we mutated the His<sup>399</sup> from hKv1.3 channel to threonine. Surprisingly, MTX blocking affinity for hKv1.3\_H399T,

MOL2774

was increased around 10000 fold, the  $K_d$  value becoming identical to the one with which MTX blocks hKv1.2, namely  $0.6 \pm 0.1$  nM ( $n = 7$ ) (Fig. 8B). Since 1  $\mu$ M MTX\_Y32A is inactive on current on hKv1.3 channel, we calculated the change in the coupling energy of this interaction assuming the  $K_d$  being between 100  $\mu$ M and 1 mM. With these approximations mutant cycle analysis show a strong change in the coupling energy (3.21 kcal/mol if we assume the  $K_d$  of hKv1.3 and MTX\_Y32A as being 100  $\mu$ M, and 1.84 kcal/mol if we assume the  $K_d$  being 1 mM) between Thr<sup>399</sup> and Tyr<sup>32</sup> suggesting that these amino acids come in very close proximity with each other, and that this position is crucial for channel recognition and interaction (Fig. 8C).



## DISCUSSION

Our work aimed to characterize the interaction of MTX with hKv1.2 and hIKCa1 channels. We report that basic  $\text{pH}_o$  values does influence the block of MTX on current through hKv1.2 channels a little, whereas acidic  $\text{pH}_o$  does not interfere with MTX blocking activity at all. Several binding sites were identified and a docking model was proposed. Additionally, common binding sites of MTX for hKv1.2, hKv1.3 and hIKCa1 channels were found.

Several reports have shown that the  $\text{pH}_o$  can influence the blocking affinity of pore blocking peptides (Deutsch et al., 1991; Perez-Cornejo et al., 1998; Bretschneider et al., 1999; Thompson and Begenisich, 2000; Wrisch and Grissmer, 2000). Moreover, we reported that MTX blocks hIKCa1 channels in a  $\text{pH}_o$  dependent manner having lower binding affinities in Ringer solution with  $\text{pH}_o$  6.2, 8.3, and 9.1 compared to measurements done at  $\text{pH}_o$  7.4 (Visan et al., 2004). We reported that the  $\text{pH}_o$  dependence at low  $\text{pH}_o$  was due to the presence of a histidine in the pore region of hIKCa1 channels (position 236) (Fig. 1A) which probably becomes protonated, and thus, might repel a positively charged amino acid from the toxin. However, in Ringer solution with high  $\text{pH}_o$  values, the  $\text{pH}_o$  dependency of the block can not be explained through the protonation of an amino acid, but rather through a slight conformational change of the toxin that might make it fit worse in the channels pore, and/or a partial loss of the exposed positively charged amino acids from the toxin that might interact with the negative charges from the channel (Kharrat et al., 1996). This theory is confirmed by our present study since the block of MTX on current through hKv1.2 channels is not  $\text{pH}_o$  dependent at  $\text{pH}_o$  6.2, and shows a very weak  $\text{pH}_o$  dependency

MOL2774

only at  $pH_o$  9.1. It seems that the lack of a protonable amino acid in the pore region of hKv1.2 (Fig. 1A) channels makes the MTX block insensitive to  $pH_o$  changes towards acidic values. However, the conformational changes of the toxin at higher  $pH_o$  values confirmed by CD spectroscopy analysis (Kharrat et al., 1996) are also sensed by the hKv1.2 channel, although to a lesser extent as by hKCa1 channel, leading to a weaker block of the modified MTX. Moreover, the comparative study made with CTX demonstrate that only MTX block is affected by the  $pH_o$  changes, CTX block on current through both hKv1.2 and hKCa1 channels being not  $pH_o$  dependent.

Studies made by now on toxin-channel interaction (Hidalgo and MacKinnon, 1995; Aiyar et al., 1996; Rauer et al., 1999, 2000; Wrisch and Grissmer, 2000) indicate that all the investigated peptide toxins have 2-3 amino acids essential for binding, namely one lysine that protrudes into the channel pore, and one or two other amino acids that are anchoring the toxin and stabilize the interaction (usually arginines or lysines). Using the thermodynamic mutant cycle analysis, and an approximate toxin docking into hKv1.2 channel, we identified six amino acid pairs that seems to be involved in channel recognition and/or the stabilization of MTX-hKv1.2 channel interaction. The docking was made using the distances estimated through the mutant cycle analysis. They indicated the orientation of the toxin in the channel and allowed us to perform an approximate fitting of MTX into the hKv1.2 channel vestibule. An homology model of KcsA and KvAP channels was used, with the presumption that the external vestibule is structurally similar between these channels and the family of mammalian Kv channels. The drastic loss in affinity of MTX\_K23A mutant for both hKv1.2 (Fig. 5A) and hKCa1 channels (Castle et al., 2000), the proximity of Lys<sup>23</sup> to Val<sup>381</sup> revealed by the mutant cycle analysis, and the computer simulations made by Fu et al. (2002), indicate that Lys<sup>23</sup> (green) is the pore protruding amino acid that

MOL2774

interacts with the GYGD motif of the potassium channels, and corresponds to Lys<sup>27</sup> in AgTx2, CTX, and KTX (Hidalgo and MacKinnon, 1995; Rauer et al., 2000; Aiyar et al., 1996) (Fig. 9). The mutant cycle analysis also confirms that Tyr<sup>32</sup> (violet) is in very close proximity with Val<sup>381</sup> from hKv1.2 channel (orange) (His<sup>399</sup> in hKv1.3 channel), and probably, together with Lys<sup>23</sup>, they form the “functional dyad” of MTX. Our data additionally indicate a strong change in coupling energy between Lys<sup>7</sup> (red) and Asp<sup>363</sup> (yellow), and Glu<sup>355</sup> (blue) from one channel subunit, and Val<sup>381</sup> (orange), probably, from the next channel subunit, suggesting a distance smaller than 5 Å between Lys<sup>7</sup> and these amino acids (Fig. 9). These interactions should tilt the MTX, and bring the Lys<sup>27</sup> (green) close to the Glu<sup>355</sup> (blue) and/or Asp<sup>363</sup> (yellow) from the next subunit (Fig. 9).

Using mutant cycle analysis we also found a strong change in coupling energy (0.92 kcal/mol) between Arg<sup>14</sup> and Glu<sup>355</sup> (Fig. 5B). However, we must keep in mind that the point mutation of Arg<sup>14</sup> to glutamine changes the disulfide bridge organization of MTX towards the Pi1/HsTx1 pattern which leads to a slightly modification of the 3D structure of the peptide (Fajloun et al., 2000). Since Lys<sup>27</sup> seems to be important in toxin-channel interaction (Fu et al., 2002), it could be that a change in the 3D structure of MTX\_R14Q as the one described by Fajloun et al. (2000) for MTX\_K15Q, might place this amino acid in a different position, and thus, might alter an important electrostatic contact. Assuming that the mutant cycle analysis is reliable when there are no conformational changes of the peptide and the channel, we will consider the 5 Å distance between Arg<sup>14</sup> and Glu<sup>355</sup> as being an incorrect estimation.

Comparing the amino acid sequence of hKv1.2, and hIKCa1 channels, we observe that three of the amino acids involved in MTX binding are conserved in both channels, namely the Tyr<sup>377</sup> and Asp<sup>379</sup> from the GYGD motif, and the Asp<sup>363</sup> (Fig.

MOL2774

1A). Val<sup>381</sup> from the hKv1.2 channel corresponds to His<sup>399</sup> in the hKv1.3 channel, and since this histidine makes the hKv1.3 channel insensitive to MTX block we presume that this position has a key role for MTX recognition. This position seems to be a hydrophobic amino acid like valine or threonine to make the channel MTX sensitive.

One might speculate about the role of Glu<sup>355</sup> in hKv1.2 channels in the toxin-channel interaction. Since MTX blocks both hKv1.2, and hKv1.3\_H399T channels with the same potency, and this amino acid is not conserved in the two channels, being replaced by an uncharged amino acid in hKv1.3\_H399T channels, one could argue that this position in hKv1.2 channel might either not be important in MTX binding or might uncover a negative interaction that is the same in both channel mutants. The mutation in the toxin might obviate this negative interaction resulting in an apparent coupling energy.

Although the role of Glu<sup>355</sup> from hKv1.2 channels in MTX-hKv1.2 channel interaction might not be clear, it is still possible that this position is important in the fine pharmacological discriminations between hKv1.2 and hKCa1 channels, and could possibly explain why slight modifications of MTX structure (induced for example by Ringer solution with basic pH<sub>o</sub>) can be better sensed by hKCa1 than by hKv1.2 channels, causing higher loss in affinity in the first case. This Glu<sup>355</sup> might stabilize MTX-hKv1.2 channels interaction, and make it less sensitive to structural alterations of toxin and/or channel (Visan et al, 2004).

*Conclusions.* Our findings suggest similarities in MTX binding to hKv1.2, hKCa1, and hKv1.3 channels. We report that MTX occludes the pore region of these channels by establishing strong interactions between Lys<sup>23</sup> and the GYGD motif, Tyr<sup>32</sup>- Val<sup>381</sup>, Lys<sup>7</sup>- Asp<sup>363</sup>, Lys<sup>7</sup>- Val<sup>381</sup> from hKv1.2 channel or the correspondent amino acids from the other channels. The other interactions that Lys<sup>7</sup> and/or Lys<sup>27</sup> makes with Glu<sup>355</sup> are

MOL2774

not essential, since the replacement of Glu<sup>355</sup> with a neutral amino acid weakly affect toxin-channel binding affinity. However, the amino acid situated in this position might be responsible for a better stabilization of the interaction and might explain the pH<sub>o</sub> sensitivity of MTX block on current through hKCa1 versus hKv1.2 channels. Our work describing the amino acids involved in complex formation, localizes the regions of binding, and by the calculated energies of interaction, makes estimations on the distances that lie between the interacting amino acids of MTX and different potassium channels. Through the topological information of these toxin-channels interactions that our study brings, these data might be helpful for future drug design studies.

## References

Aiyar J, Rizzi JP, Gutman GA and Chandy KG (1996) The signature sequence of voltage-gated potassium channels projects into the external vestibule. *J Biol Chem* **271**(49):31013-31016.

Avdonin V, Nolan B, Sabatier J-M, De Waard M and Hoshi T (2000) Mechanisms of maurotoxin action on Shaker potassium channels. *Biophys J* **79**:776-787.

Bretschneider F, Wrisch A, Lehmann-Horn F and Grissmer S (1999) External tetraethylammonium as a molecular caliper for sensing the shape of the outer vestibule of potassium channels. *Biophys J* **76**(5):2351-2360.

Castle NA, London DO, Creech C, Fajloun Z, Stocker JW and Sabatier J-M (2003) Maurotoxin: a potent inhibitor of intermediate conductance  $\text{Ca}^{2+}$ -activated potassium channels. *Mol Pharmacol* **63**:409-418.

Chandy KG, Cahalan MD, Pennington M, Norton RS, Wulff H, and Gutman GA (2001) Potassium channels in T lymphocytes: toxins to therapeutic immunosuppressants. *Toxicon* **39**:1269-1276

Coleman SK, Newcombe J, Pryke J and Dolly JO (1999) Subunit composition of Kv1 channels in human CNS. *J Neurochem* **73**(2): 849-858.

MOL2774

Deutsch C, Price M, Lee S, King VF and Garcia ML (1991) Characterization of high affinity binding sites for charybdotoxin in human T lymphocytes. Evidence for association with the voltage-gated K<sup>+</sup> channel. *J Biol Chem* **266**(6):3668-3674.

Dodson PD, Billups B, Rusznak Z, Szucs G, Barker MC and Forsythe ID (2003) Presynaptic rat Kv1.2 channels suppress synaptic terminal hyperexcitability following action potential invasion. *J Physiol* **550**(Pt 1):27-33.

Doyle DA, Morais Cabral J, Pfuetzner RA, Kuo A, Gulbis JM, Cohen SL, Chait BT and MacKinnon R (1998) The structure of the potassium channel: molecular basis of K<sup>+</sup> conduction and selectivity. *Science* **280**(5360):69-77.

Elliot JI and Higgins CF (2003) IKCa1 activity is required for cell shrinkage, phosphatidylserine translocation and death in T lymphocytes apoptosis. *EMBO Rep* **4**(2):189-194.

Fajloun Z, Mosbah A, Carlier E, Mansuelle P, Sandoz G, Fathallah M, Luccio E, Devaux C, Rochat H, Darbon C, De Waard M and Sabatier J-M (2000) Maurotoxin versus Pi1/HsTx1 scorpion toxins. Toward new insights in the understanding of their distinct disulfide bridge patterns. *J Biol Chem* **275**(50):39394-39402.

Fu W, Cui M, Briggs JM, Huang X, Xiong B, Zhang Y, Luo X, Shen J, Ji R and Chen K (2002) Brownian dynamics simulations of the recognition of the scorpion toxin maurotoxin with the voltage-gated potassium ion channels. *Biophys J* **83**:2370-2385.

MOL2774

Ghanshani S, Wulff H, Miller MJ, Rohm H, Neben A, Gutman GA, Cahalan MD and Chandy KG (2000) Up-regulation of the IKCa1 potassium channel during T-cell activation. Molecular mechanism and functional consequences. *J Biol Chem* **275**(47):37137-37149.

Grissmer S, Nguyen AN and Cahalan MD (1993) Calcium-activated potassium channels in resting and activated human T lymphocytes. Expression levels, calcium dependence, ion selectivity, and pharmacology. *J Gen Physiol* **102**(4):601-630.

Hamill O P, Marty A, Neher E, Sakmann B and Sigworth F J (1981) Improved patch-clamp techniques for high-resolution current recording from cells and cell-free membrane patches. *Pflügers Arch* **391**: 85-100.

Hidalgo P and MacKinnon R (1995) Revealing the architecture of a K<sup>+</sup> channel pore through mutant cycles with a peptide inhibitor. *Science* **268**: 307-310.

Ishii TM, Silvia C, Hirschberg B, Bond CT, Adelman JP and Maylie J (1997) A human intermediate conductance calcium-activated potassium channel. *Proc Natl Acad Sci USA* **94**: 11651-11656.

Jager H, Dreker T, Buck A, Giehl K, Gress T, Grissmer S (2004) Blockage of intermediate-conductance Ca<sup>2+</sup>-activated K<sup>+</sup> channels inhibit human pancreatic cancer cell growth in vitro. *Mol Pharmacol* **65**(3):630-638.



MOL2774

Jiang Y, Lee A, Chen J, Ruta V, Cadene M, Chait BT, MacKinnon R (2003) X-ray structure of a voltage-dependent K<sup>+</sup> channel. *Nature* **423**(6935):33-41.

Khanna R, Chang MC, Joiner WJ, Kaczmarek LK and Schlichter LC (1999) hSK4/hIK1, a calmodulin-binding K<sub>Ca</sub> channel in human T lymphocytes. Roles in proliferation and volume regulation. *J Biol Chem* **274**(21):14838-14849.

Kharrat R, Mabrouk K, Crest M, Darbon H, Oughideni R, Martin-Eauclaire M-F, Jaquet G, El Ayeb M, Van Rietschoten J, Rochat H and Sabatier J-M (1996) Chemical synthesis and characterization of maurotoxin, a short scorpion toxin with four disulfide bridges that acts on K<sup>+</sup> channels. *Eur J Biochem* **242**:491-498.

Kharrat R, Mansuelle P, Sampieri F, Crest M, Oughideni R, Van Rietschoten J, Martin-Eauclaire MF, Rochat H and El Ayeb M (1997) Maurotoxin, a four disulfide bridge toxin from *Scorpio maurus* venom: purification, structure and action on potassium channels. *FEBS Lett* **406**(3):284-290.

Kohler R, Degenhardt C, Kuhn M, Runkel N, Paul M and Hoyer J (2000) Expression and function of endothelial Ca(2+)-activated K(+) channels in human mesenteric artery: A single-cell reverse transcriptase-polymerase chain reaction and electrophysiological study in situ. *Circ Res* **87**(6):496-503.

Lambert P, Kuroda H, Chino N, Watanabe TX, Kimura T and Sakakibara S (1990) Solution synthesis of charybdotoxin (ChTX), a K<sup>+</sup> channel blocker. *Biochem Biophys Res Commun* **170**(2):684-690.

MOL2774

Lecomte C, Ben Khalifa R, Martin-Eauclaire MF, Kharrat R, El Ayeub M, Darbon H, Rochat H, Crest M and Sabatier J-M (2000) Maurotoxin and the Kv1.1 channel: voltage-dependent binding upon enantiomerization of the scorpion toxin disulfide bridge Cys31-Cys34. *J Pept Res* **55**(3):246-254.

Logsdon N, Kang J, Togo JA, Christian EP and Aiyar J (1997) A novel gene, hKCa4, encodes the calcium-activated potassium channel in human T lymphocytes. *J Biol Chem* **272**(52): 32723-32726.

Merrifield RB (1986) The solid phase peptide synthesis. *Science* **232**:341-347.

Monaghan MM, Trimmer JS and Rhodes KJ (2001) Experimental localization of Kv1 family voltage-gated K<sup>+</sup> channel alpha and beta subunits in rat hippocampal formation. *J Neurosci* **21**(16):5973-5983.

Pena TL and Rane SG (1999) The fibroblast intermediate conductance K(Ca) channel, FIK, as a prototype for the cell growth regulatory function of the IK channel family. *J Membr Biol* **172**(3): 249-257.

Perez-Cornejo P, Stampe P and Begenisich T (1998) Proton probing of the charybdotoxin binding site of Shaker K<sup>+</sup> channels. *J Gen Physiol* **111**(3):441-450 .

MOL2774

Rane SG (2000) The growth regulatory fibroblast IK channel is the prominent electrophysiological feature of rat prostatic cancer cells. *Biochem Biophys Res Commun* **269**(2):457-463 .

Rauer H and Grissmer S (1996) Evidence for an internal phenylalkylamine action on the voltage-gated potassium channel Kv1.3. *Mol Pharmacol* **50**: 1625-1634.

Rauer H, Lanigan MD, Pennington MW, Aiyar J, Ghanshani S, Cahalan MD, Norton RS and Chandy KG (2000) Structure-guided transformation of charybdotoxin yields an analog that selectively targets Ca(2+)-activated over voltage-gated K(+) channels. *J Biol Chem* **275**(2): 1201-1208.

Schreiber G and Fersht AR (1995) Energetics of protein-protein interactions: analysis of the barnase-barstar interface by single mutations and double mutant cycles. *J Mol Biol* **248**(2):478-486.

Thompson J and Begenisich T (2000) Electrostatic interaction between charybdotoxin and a tetrameric mutant of Shaker K(+) channels. *Biophys J* **78**(5):2382-2391.

Tytgat J, Chandy KG, Garcia ML, Gutman GA, Martin-Eauculaire MF, van der Walt JJ and Possani LD (1999) A unified nomenclature for short-chain peptides isolated from scorpion venoms: alpha-KTx molecular subfamilies. *Trends Pharmacol Sci* **20**(11):444-447.

MOL2774

Vandorpe DH, Shmukler BE, Jiang L, Lim B, Maylie J, Adelman JP, Franceschi L, Cappellini MD, Brugnara C and Alper SL (1998) cDNA cloning and functional characterization of the mouse  $\text{Ca}^{2+}$ -gated  $\text{K}^{+}$  channel, mIK1. *J Biol Chem* **273**(34):21542-21553.

Visan V, Sabatier JM, Grissmer S (2004) Block of maurotoxin and charybdotoxin on human intermediate-conductance calcium-activated potassium channels (hIKCa1). *Toxicon* **43**:973-980.

Wrisch A and Grissmer S (2000) Structural differences of bacterial and mammalian  $\text{K}^{+}$  channels. *J Biol Chem* **275**(50):39345-39353.

Wulff H, Miller MJ, Hansel W, Grissmer S, Cahalan MD and Chandy KG (2000) Design of a potent and selective inhibitor of the intermediate-conductance  $\text{Ca}^{2+}$ -activated  $\text{K}^{+}$  channel, IKCa1: a potential immunosuppressant. *Proc Natl Acad Sci USA* **97**(14):8151-8156.

MOL2774

### *Footnotes*

This work was supported by grants from the DFG (Gr 848/8-2) and BMBF (IZKF B7).

This work was partially presented as a poster: Visan V, Sabatier J-M, Grissmer S (2004) Is the block of current through voltage-gated Kv1.2 channels by maurotoxin pH<sub>o</sub> dependent? *Biophysical J* **86**(1):538a

Reprint requests should be addressed to: Prof. Dr. Stephan Grissmer, Department of Applied Physiology, University of Ulm, Albert-Einstein-Allee 11, D-89081 Ulm, Germany, Tel.: +49 (0)731-502 3253; Fax: +49 (0)731-502 3237, Email: [stephan.grissmer@medizin.uni-ulm.de](mailto:stephan.grissmer@medizin.uni-ulm.de)

## Legends for Figures

**Fig. 1.** Alignment of channels and toxins. A, amino acid alignment of different potassium channel sequences in the putative pore region. The highlighted positions are important in MTX binding; B, alignment of the amino acid sequences of MTX and CTX.

**Fig. 2.** MTX is a potent blocker of hKv1.2 and hKCa1 channels, but not of hKv1.3 channels. (A) Potassium currents through hKv1.2 channel in the absence and the presence of 1 nM MTX. Currents were elicited using an use-dependence pulse protocol, consisting of 10 depolarising voltage steps of 200 ms, from the membrane potential, -80 to + 40 mV, repeated every second. The dose-response curve revealed a  $K_d$  of  $0.7 \pm 0.1$  nM ( $n = 5$ ). (B) Potassium currents through hKCa1 channel in the absence and the presence of 5 nM MTX. Currents were elicited using 400 ms voltage ramps from -120 to 0 mV, repeated each 15 seconds. The dose-response curve revealed a  $K_d$  of  $4.3 \pm 0.3$  nM ( $n = 4$ ). (C) Potassium currents through hKv1.3 channel in the absence and the presence of 5  $\mu$ M MTX. Currents were elicited using voltage steps of 200 ms, from the membrane potential, -80 to + 40 mV, repeated every 40 seconds. The dose-response curve revealed a  $K_d$  of  $3.3 \pm 0.2$   $\mu$ M ( $n = 9$ ).

**Fig. 3.** pH<sub>o</sub>-dependent block of extracellularly applied MTX on currents through hKv1.2 channels. Currents were elicited by ten voltage steps of 200 ms from -80 to 40 mV, every second. Currents were measured in normal Ringer solution with pH<sub>o</sub> 6.2

MOL2774

(A), 7.4 (B), 8.3 (C), and 9.1 (D), before (control) and after application of 1 nM MTX.

**Fig. 4.** pH<sub>o</sub>-dependent block of extracellularly applied CTX on currents through hKv1.2 channels. Currents were elicited by ten voltage steps of 200 ms from -80 to 40 mV, every second. Currents were measured in normal Ringer solution with pH<sub>o</sub> 6.2 (A), 7.4 (B), 8.3 (C), and 9.1 (D), before (control) and after application of 20 nM CTX.

**Fig. 5.** K<sub>d</sub> values and calculated changes in coupling energies ( $\Delta\Delta G$ ) for wild type and mutant MTX and hKv1.2 channels. (A) K<sub>d</sub> values calculated using dose-response curves or single concentration (when K<sub>d</sub> values were bigger than 100 nM) as described in the Methods section; (B)  $\Delta\Delta G$  calculated (as described in the Methods) using the K<sub>d</sub> values of the wild type and mutant MTX and hKv1.2 channels.

**Fig. 6.** Comparative block of wild type (A) and mutant (B) MTX on currents through hKv1.2 channels. The original trace currents through hKv1.2 channels represented in the figures were measured in transiently transfected COS7 cells, and elicited by ten depolarising voltage steps of 200 ms, from the membrane potential, -80 mV, to +40 mV, every second; (C) Thermodynamic mutant cycle for the most strongly coupled pairs of residues involved in the binding of MTX to the external vestibule of hKv1.2 channels. The K<sub>d</sub> values were calculated using dose-response or single concentration (when K<sub>d</sub> values were bigger than 100 nM) as described in the Methods section. The changes in coupling energies ( $\Delta\Delta G$ ) for wild type and mutant MTX and hKv1.2

MOL2774

channels were calculated using the  $K_d$  values of the wild type and mutant MTX and hKv1.2 channels (see the Methods section).

**Fig. 7.** Comparative block of wild type (A) and mutant (B) MTX on currents through hIKCa1 channels. The original trace currents through hIKCa1 channels represented in the figures were measured in transiently transfected COS7 cells, and elicited by 1  $\mu$ M  $[Ca^{2+}]_i$  and 400 ms voltage ramps, from -120 mV to 0 mV, every 15 seconds; (C) Thermodynamic mutant cycle performed for MTX\_Lys<sup>7</sup> and hIKCa1\_Asp<sup>239</sup>. The  $K_d$  values were calculated using dose-response or single concentration (when  $K_d$  values were bigger than 100 nM) as described in the Methods section. The changes in coupling energy ( $\Delta\Delta G$ ) for wild type and mutant MTX and hIKCa1 channels was calculated using the  $K_d$  values of the wild type and mutant MTX and hIKCa1 channels (see the Methods section).

**Fig. 8.** Comparative block of MTX on currents through wild type (A) and mutant (B) hKv1.3 channels. The original trace currents through hKv1.3 channels represented in the figures were measured in transiently transfected COS7 cells, and elicited by 200 ms depolarising voltage steps, from the membrane potential -80 mV to +40 mV, every 40 seconds; (C) Thermodynamic mutant cycle performed for MTX\_Tyr<sup>32</sup> and hKv1.3\_His<sup>399</sup>. The  $K_d$  values were calculated using dose-response or single concentration (when  $K_d$  values were bigger than 100 nM) as described in the Methods section. The changes in coupling energy ( $\Delta\Delta G$ ) for wild type and mutant MTX and hKv1.3 channels was calculated using the  $K_d$  values of the wild type and mutant MTX and hKv1.3 channels (see the Methods section).



MOL2774

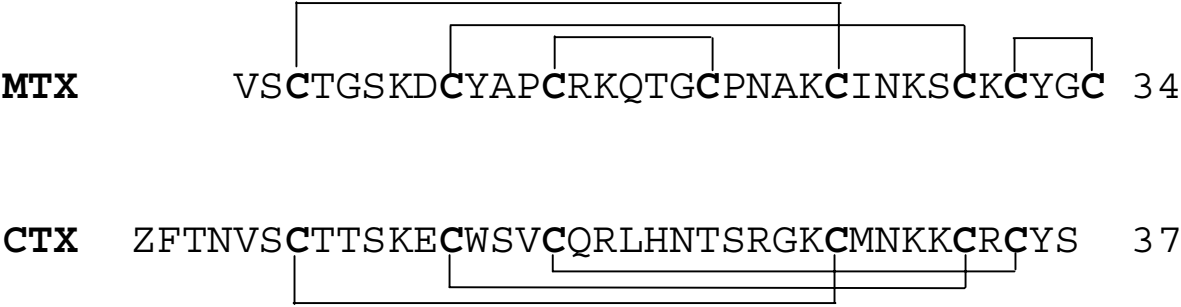
**Fig. 9.** Docking of MTX into a homology model of hKv1.2 channel. The docking configuration is shown as top (A), and side (B) view. The homology structure of hKv1.2 channel is based on the KcsA and KvAP crystal structure. The channel backbone is represented in gray, while MTX is shown as green ribbons. Interacting channel amino acids are represented in blue (Glu<sup>355</sup>), yellow (Asp<sup>363</sup>), and orange (Val<sup>381</sup>) as space filled cartoons, while their interacting toxin partners are represented in cyan (Arg<sup>14</sup>), red (Lys<sup>7</sup>), green (Lys<sup>23</sup>), and violet (Tyr<sup>32</sup>) space filled cartoons. The figure was made using RasMol v2.

1

A

<b>KcsA</b>	50	AERGAP	GAQLITYP	RALWWSVETATTVG	YGDLY	PVTLWGR	89
<b>Shaker</b>	419	AEAGSEN	SFFKSIP	DAFWWAVVTMTTVG	YGDMT	PVGFWGK	458
<b>KvAP</b>	171	VEYPDP	NSSIKSVF	DALWWAVVTMTTVG	YGDVV	PATPIGK	210
<b>hIKCa1</b>	226	AERQAV	NAT-GHLS	DTLWLIPITFLTIG	YGDVV	PGTMWGK	264
<b>hKv1.2</b>	349	AEADER	ESQFPSIP	DAFWWAVVSMTTVG	YGDMV	PTTIGGK	388
<b>hKv1.3</b>	369	AEADDPT	TSGFSSIP	DAFWWAVVTMTTVG	YGDMH	PVTIGGK	406

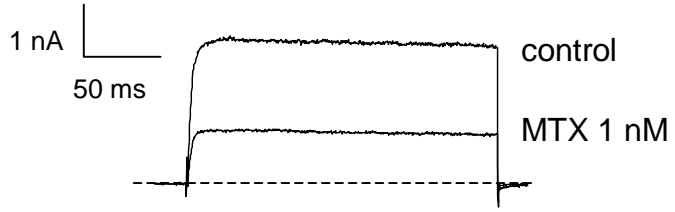
B



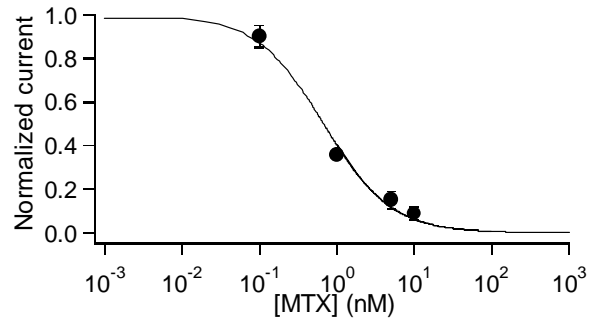
2

A

hKv1.2

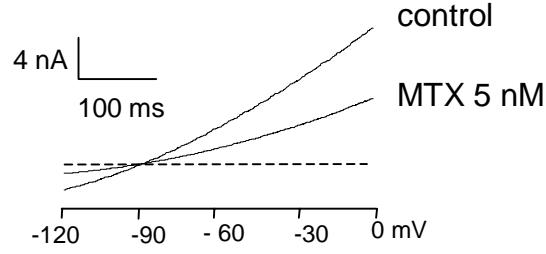


$$K_d = 0.7 \pm 0.1 \text{ nM}$$

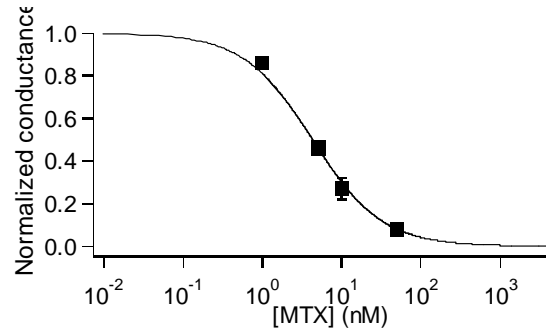


B

hKCa1

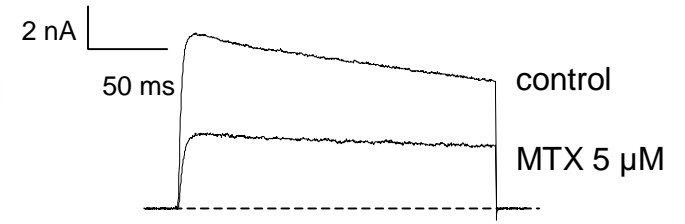


$$K_d = 4.3 \pm 0.3 \text{ nM}$$

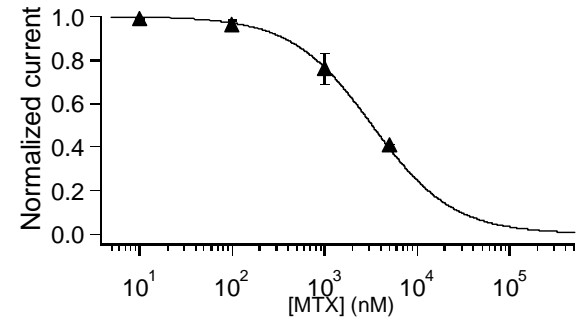


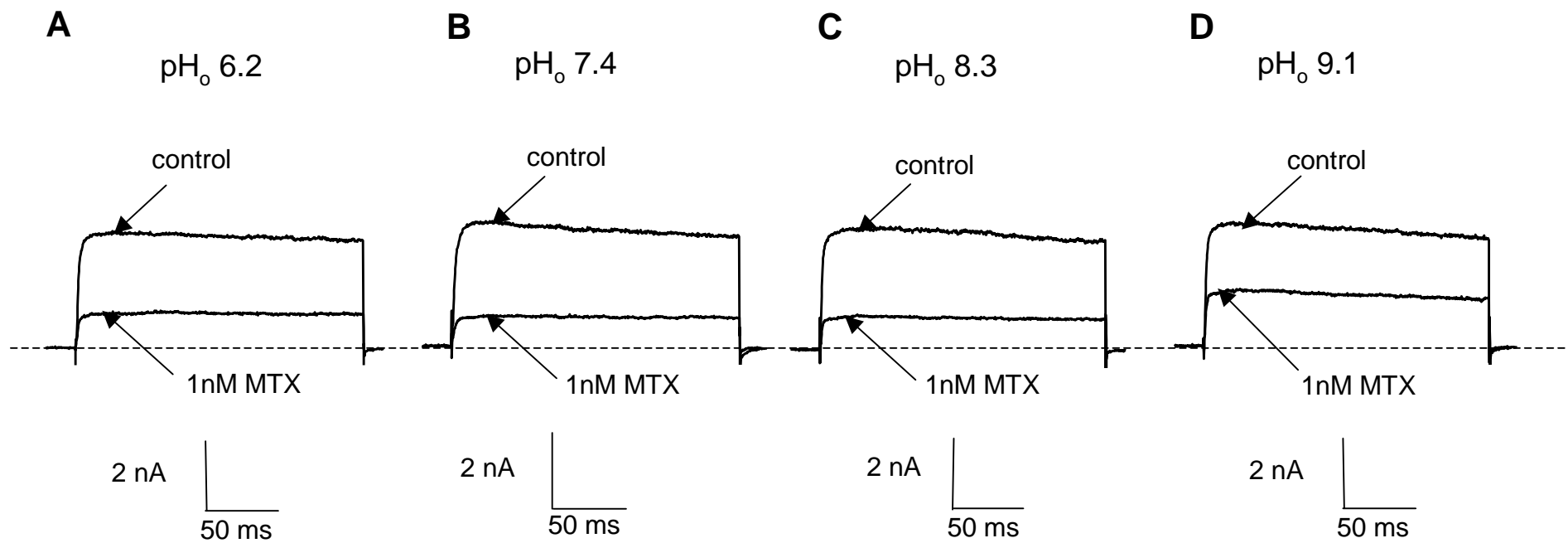
C

hKv1.3

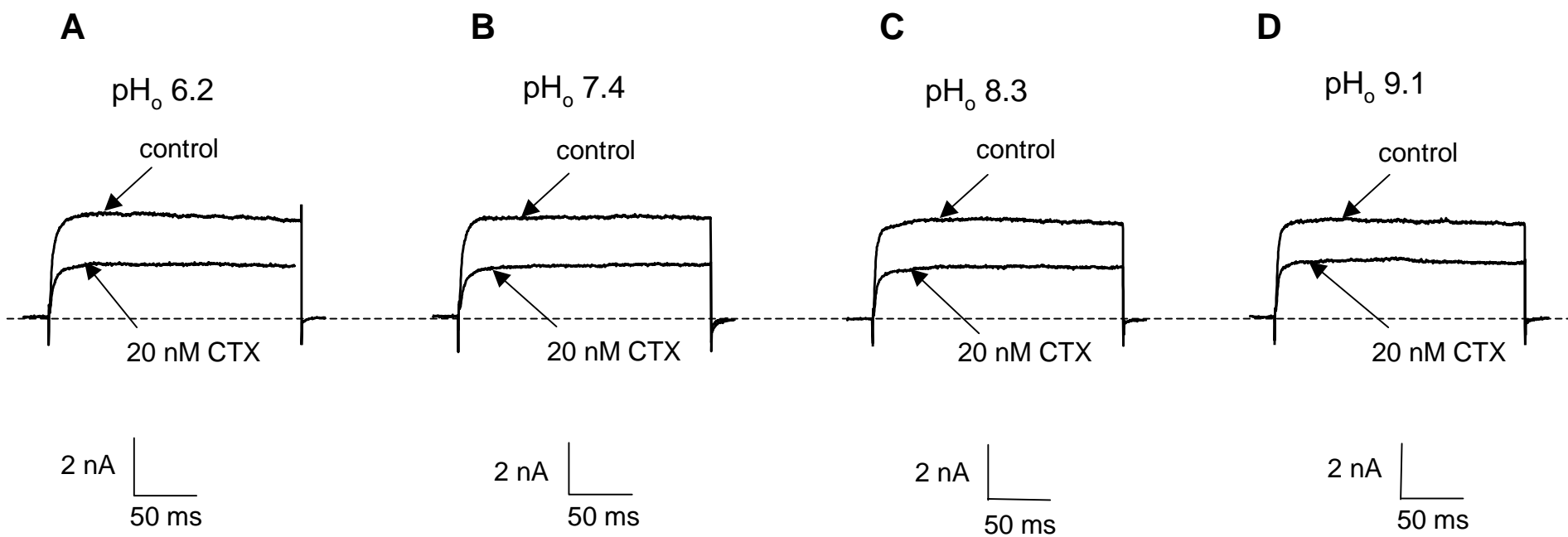


$$K_d = 3.3 \pm 0.2 \text{ μM}$$



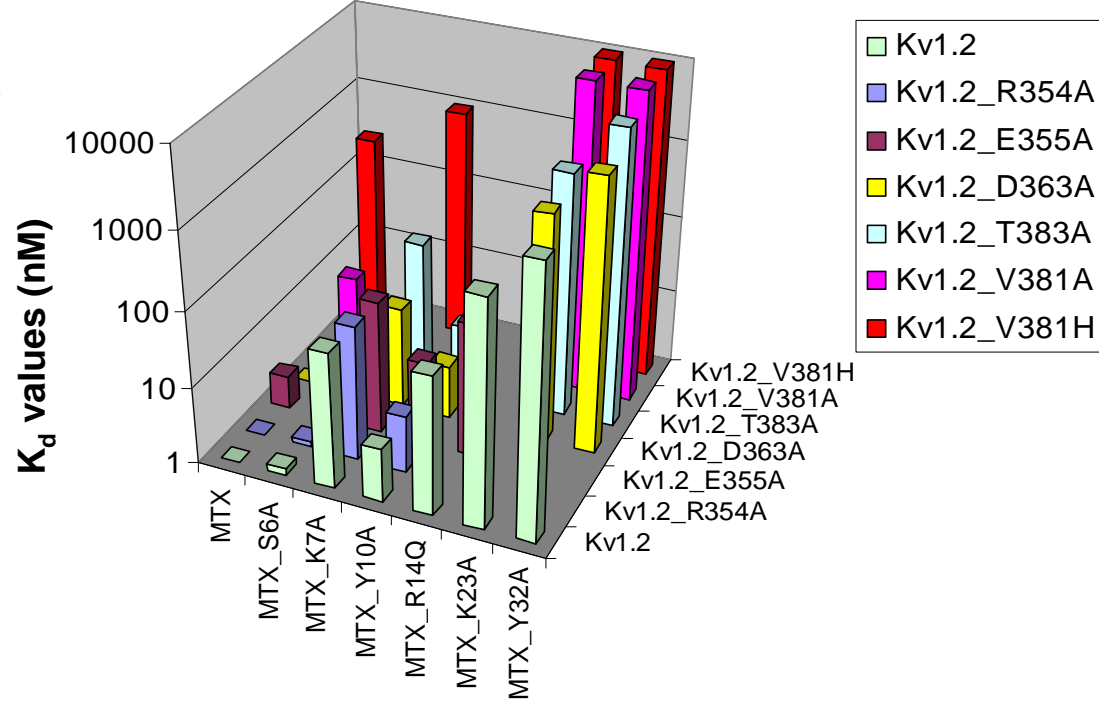


4

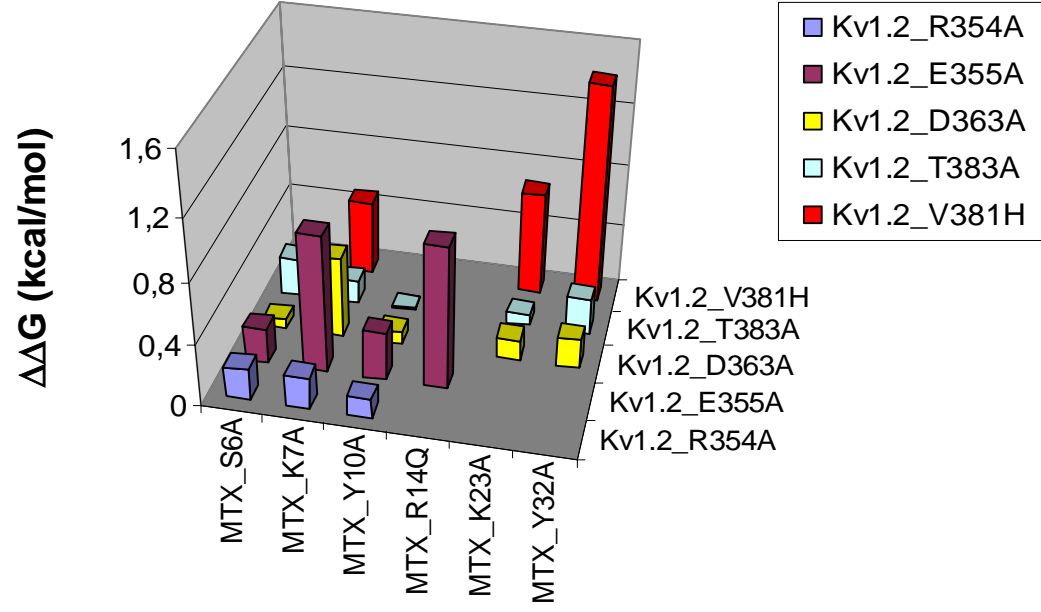


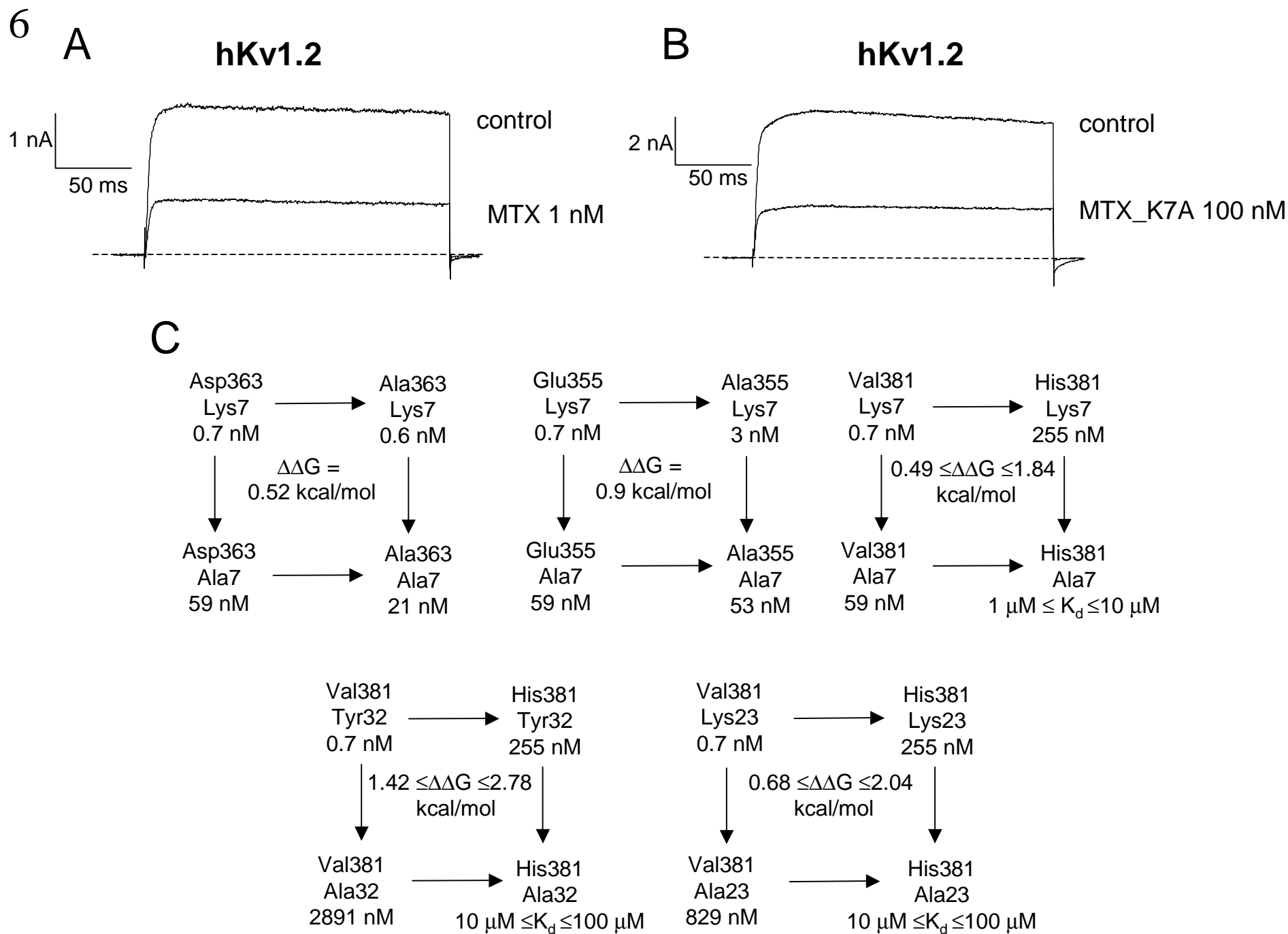
5

A



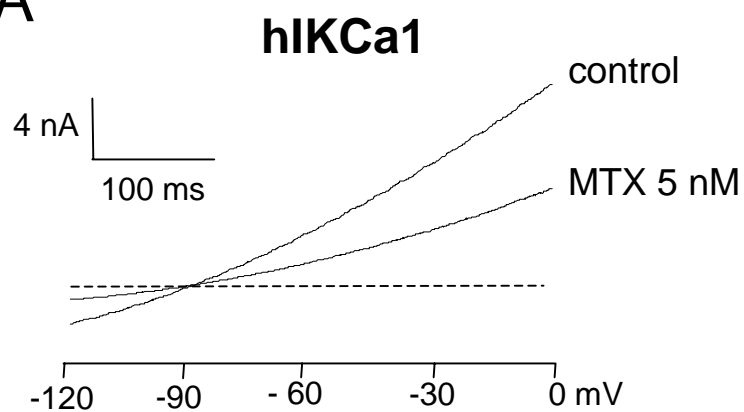
B



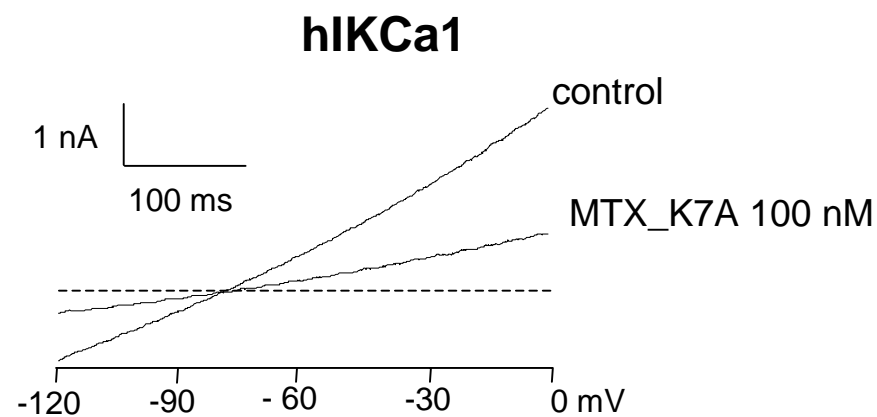


7

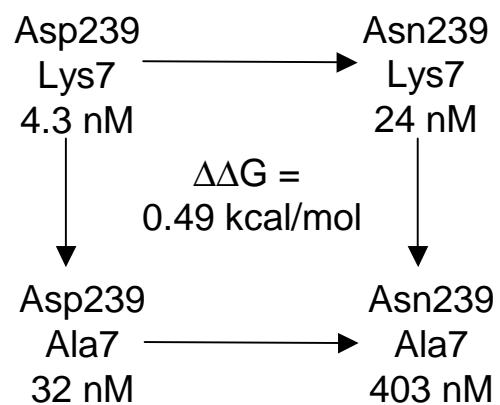
A



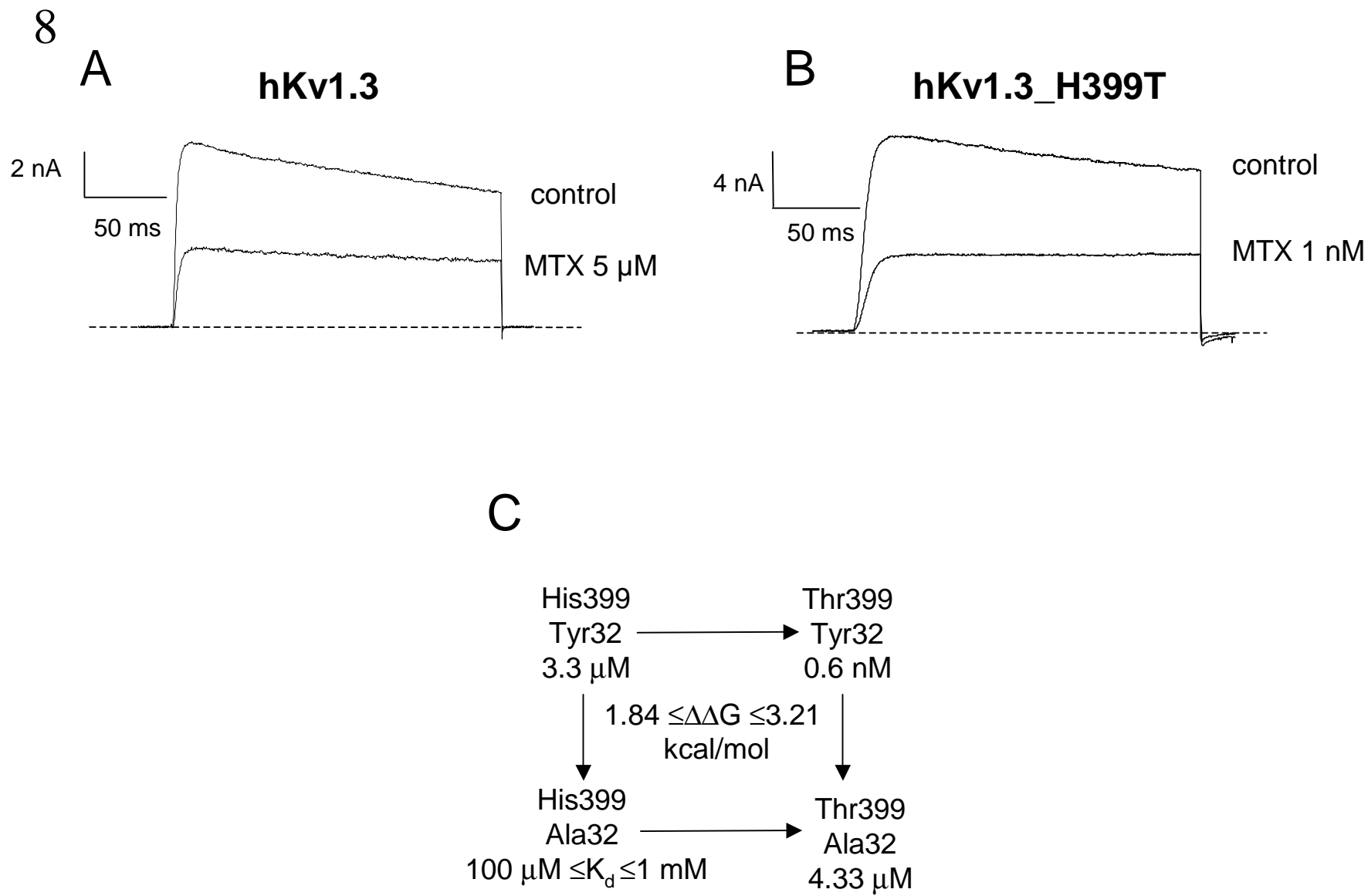
B



C

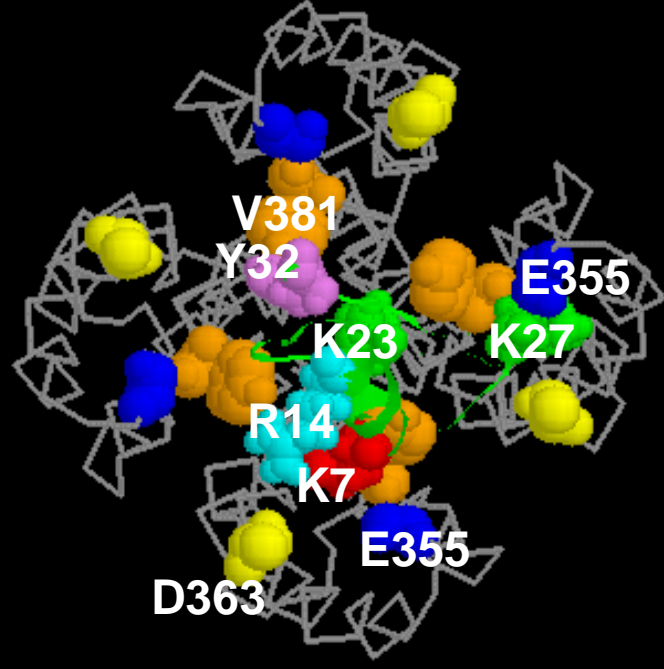






9

A



B

